ISSN 1061-3862, International Journal of Self-Propagating High-Temperature Synthesis, 2019, Vol. 28, No. 1, pp. 18–27. © Allerton Press, Inc., 2019.

Catalytic Activity of KOH–CaO–Al_2O_3 Nanocomposites in Biodiesel Production: Impact of Preparation Method[1]

H. Nayebzadeh[a, *, **], N. Saghatoleslami[a], M. Haghighi[b, c], and M. Tabasizadeh[d]

[a] *Department of Chemical Engineering, Faculty of Engineering, Ferdowsi University of Mashhad, Mashhad, P.O. Box 9177948974 Iran*

[b] *Chemical Engineering Faculty, Sahand University of Technology, Sahand New Town, Tabriz, P.O. Box 51335-1996 Iran*

[c] *Reactor and Catalysis Research Center (RCRC), Sahand University of Technology, Sahand New Town, Tabriz, P.O. Box 51335-1996 Iran*

[d] *Department of Biosystems Engineering, Faculty of Agriculture, Ferdowsi University of Mashhad, Mashhad, P.O. Box 9177948974 Iran*

**e-mail: hamed.nayebzadeh@mail.um.ac.ir*

***e-mail: h.nayebzadeh@yahoo.com*

Received May 14, 2018; revised June 14, 2018; accepted September 7, 2018

Abstract—$CaO–Al_2O_3$ mixed oxides were prepared by different preparation methods – such as sol–gel, co-precipitation, impregnation, and MW-assisted solution combustion synthesis (M-SCS) – and then impregnated with KOH to examine their activity in transesterification of canola oil to biodiesel. Synthesized nanocomposites were characterized by XRD, FTIR, BET/BJH, and SEM/EDX. The mixed oxides, except those prepared by M-SCS method, exhibited a nearly amorphous structure with some diffraction peaks of calcium oxide. Due to high combustion temperature during the M-SCS process, Ca ions could diffuse into the alumina lattice to form $CaAl_2O_4$. But upon impregnation with KOH, the former transformed to $Ca_{12}Al_{14}O_{33}$. The $KOH/Ca_{12}Al_{14}O_{33}$ nanocatalyst prepared by M-SCS method exhibited better basicity, mean pore size, and activity, as well as highest Ca/Al and K/Al ratios. In the presence of this catalyst, around 86% of canola oil were converted to biodiesel in the transesterification reaction carried out at 65°C, methanol/oil molar ratio 12 : 1, 4 wt % catalyst, 4 h. Such parameters seem appropriate for industrial application. The M-SCS method is technically simple, cost effective, time/energy saving and requires no further thermal treatment.

Keywords: MW-assisted solution combustion synthesis, calcium aluminate, nanocatalysts, biodiesel, transesterification

DOI: 10.3103/S1061386219010102

1. INTRODUCTION

Over recent years, decreasing crude oil sources, increasing greenhouse gas emissions, and ecological warming have encouraged scientists to devote a search for alternative fuels. Biodiesel has become very popular as an alternative for fossil fuel due to its renewability, biodegradability, non-toxicity, low emission profiles, and excellent lubrication behavior. Biodiesel consists of fatty acid methyl ester (FAME) derived by esterification and transesterification of free fatty acid (FFA) and triglyceride with methanol [1]. The utilization of waste frying oil (WFO) as a feedstock for new-generation biofuels will not cause any controversy regarding the competition of fuel with human food source; neither will it be detrimental to the environment, particularly in comparison with the feedstock utilized for first-generation biofuels as raw vegetable oils. Moreover, the use of WFO certainly reduces the cost of biodiesel production and it is the main driving force for studies in the field. However, WFO normally contains a lot of FFA, which creates a problem for biodiesel production using conventional homogeneous alkali catalysts such as NaOH and KOH. These catalysts have some setback such as solubility in the reaction medium, reaction with FFA to form soap, several expensive separation stages, purification/neutralization steps, and large amount of alkaline wastewater. To avoid the above problems and to reduce the production cost, environmentally friendly heterogeneous catalysts can be used as a substitute [2, 3].

For use in transesterification reactions, solid-base catalysts have been proposed. However, WFO cannot be transesterified under mild conditions in the presence of heterogeneous catalysts: usually high molar ratios of alcohol to oil, large amounts of catalyst, high temperatures, and long reaction times are needed in

[1] The article is published in the original.

order to overcome diffusion-related restrictions caused by the presence of three phases: catalyst, alcohol, and oil. Therefore, the use of catalyst supports that would provide high specific surface area and large pores for incorporation of active species have been suggested [4]. Komintarachat et al. [5] evaluated the capacity of porous support materials such as alumina, silica, titania, and zinc oxide for synthesized WO_x catalysts, based on FAME yields. As a result, Al_2O_3 was found to be a best candidate for the role of porous support due to its higher surface area. Alumina was utilized as a support for various materials such as metal hydroxides [6–8], alkaline metal oxides [9, 10], and transition metal oxides [11, 12]. Among these, CaO [13–17] and KOH [18–22] were widely used for biodiesel production. The basicity of calcium oxide is as high as that of barium and strontium oxide and its sources such as calcium carbonate, calcium acetate, and calcium nitrate are less expensive and toxic [23, 24].

Different results for CaO and KOH loading in alumina and best methods for preparing the catalysts have been reported in the literature. Catalysts in question can obtained by using such procedures as co-precipitation [25], impregnation [13, 16], sol–gel [24, 26] and hydrothermal [27, 28]. However, preparing the catalyst with high-purity oxide powders with the above techniques has not received much attention because of expensive raw materials and multistage processing. The has emerged as An attractive way to production of homogeneous, high-purity, and crystalline oxide powders turned to be the technique of solution combustion synthesis (SCS) [29, 30]. However, the potential of SCS-produced catalysts for biodiesel production has not been studied so far.

In this study, we comparatively examined the best synthetic procedures for the preparation of CaO–Al_2O_3 mixed oxides as a support for the KOH impregnated as an active component of thus prepared heterogeneous catalyst for methanolysis of canola oil in the biodiesel production process.

2. EXPERIMENTAL

2.1. Preparation of Catalysts

CaO–Al_2O_3 (1 : 1 mole ratio) to be used as supported catalyst was synthesized in four routes: impregnation, co-precipitation, sol–gel, and SCS. In all cases, the solutions of 0.5 M $Al(NO_3)_3 \cdot 9H_2O$ (hereinafter **A**) and 0.5 M $Ca(NO_3)_2$ (**B**) were prepared.

In impregnation technique, 40 mL of solution **A** was first stirred at 80°C for 2 h and then calcined at 718°C for 5 h to form Al_2O_3. Then the obtained powder was mixed with 20 mL of solution **B** at 80°C for 2 h under total reflux. The obtained slurry was held at 100°C overnight in order to remove the water. Finally, the mix was calcined at 718°C for 5 h in air to obtain catalyst CA-**I** [16].

In co-precipitation method, 40 mL of solution **A** and 20 mL of solution **B** were mixed and vigorously stirred at 80°C for 2 h under total reflux. The solution pH was kept close to 10 by adding 1 M NH_3 solution to ensure complete precipitation. The resulting precipitates were washed with deionized water several times to neutral reaction. The washed powder was dried and calcined at the same conditions of impregnation method to obtain catalyst CA-**P**.

In sol–gel method, 40 mL of solution **A** and 20 mL of solution **B** were mixed with a required amount of citric acid to keep the pH close to 1, and the solution was refluxed at 80°C for 2 h [15]. Then the excess water was slowly evaporated to obtain gel which was dried and calcined under the earlier mentioned conditions to get catalyst CA-**S**.

To obtain CaO–Al_2O_3 by solution combustion synthesis (SCS), 40 mL of solution **A** and 20 mL of solution **B**, and a desirable amount of urea [according to propellant chemistry of Eq. (1)] were mixed in a 1000-mL beaker at 80°C to form gel. Then, the gel was placed into a microwave oven (Daewoo, Model KOC9N2TB, 900 W, 2.45 GHz). In 3 min of heating, an exothermic reaction got started, released large amount of smoke, and yielded the white foam of catalyst CA-**M**. The latter was used without further annealing.

$$\begin{aligned} &Ca(NO_3)_2 \cdot 6H_2O + 2Al(NO_3)_3 \cdot 9H_2O \\ &\quad + 6.67CO(NH_2)_2 \rightarrow CaO\text{–}Al_2O_3 \\ &+ [24 + 2 \times 6.67]H_2O + 6.67CO_2 + (6.67 + 4)N_2. \end{aligned} \quad (1)$$

KOH-containing catalysts (weight ratio 0.35) were prepared by impregnation technique. Aliquot amount of synthesized catalyst was mixed with a required amount of aqueous KOH solution at 80°C for 2 h under total reflux. Then the mix was slowly stirred at 70°C until formation of highly viscous gel that was dried and calcined as described above. Thus prepared catalysts were labeled as KCA-**I**, KCA-**P**, KCA-**S**, and KCA-**M** (cf. Table 1).

2.2. Characterization of Catalysts

The catalyst crystalline phases were characterized with XRD (UNISANTIS/XMP 300, Cu-K_α radiation). The crystallite sizes were calculated using the Scherrer equation. The active surface of functional groups in synthesized catalysts was evaluated from FTIR spectra (400–4000 cm^{-1}, Shimadzu 4300 spectrometer). Specific surface area, mean pore size, and pore volume of catalysts were determined by BET (Brunauer–Emmett–Teller) and BJH (Barrett–Joyner–Hallender) methods (Belsorp mini II BelJapan system). The basic strength of the solid bases (H^-) was determined by using Hammett indicators: bromothymol blue ($H^- = 7.2$), phenolphthalein ($H^- = 9.8$) and 2,4-dinitroaniline ($H^- = 15.0$). To measure the basicity of the catalysts, the method of Hammett titra-

Table 1. Physicochemical properties of catalysts prepared by different methods

Sample	CS[1], nm	RC[2], %	S_a, m^2/g	P_d, nm	P_v, cc/g	Base property		Yield, %
						(H^-)	mmol/g	
CA-**S**	–	–	45.32	4.30	0.192	<7.2	–	<10
CA-**M**	–	–	38.95	8.74	0.124	<7.2	–	25.1
CA-**P**	–	–	124.81	5.27	0.469	<7.2	–	<10
CA-**I**	–	–	33.74	5.86	0.138	<7.2	–	18.3
KCA-**S**	21	78.2	23.75	4.29	0.080	9.8–15	0.363	62.8
KCA-**M**	24	74.1	48.14	5.43	0.142	9.8–15	0.392	85.9
KCA-**P**	18	49.7	60.17	4.62	0.225	9.8–15	0.382	75.2
KCA-**I**	30	100	48.46	5.03	0.148	9.8–15	0.377	82.6

[1] CS crystallite size, [2] RC relative crystallinity.

tion (indicator: benzene carboxylic acid (0.02 mol/L anhydrous ethanol solution) was utilized [21, 31]. The synthesized catalysts were characterized by SEM/EDX [VP 1450 LEO microscope equipped with an electron backscatter diffraction (EDBS) accessory].

2.3. Catalyst Testing

The activity of catalysts was evaluated for transesterification of canola oil in a 250 mL glass reactor equipped with a water-cooled condenser and a magnetic stirrer. The following reaction conditions were used in all the tests: 65°C, 4 wt % of the oil, , stirring at 700 rpm, methanol/oil molar ratio 12 : 1, test duration 4 h [17]. After completing the reaction, the mix was centrifuged at 2500 rpm for 25 min, and the upper liquid phase (containing biodiesel) was heated to remove excess methanol. Finally, the biodiesel was analyzed by gas chromatography (Teif Gostar Faraz, Iran, equipped with FID detector and SUPRAWAX-280 capillary column). On each run, the 1-μL sample containing 100 μL biodiesel was dissolved in 1 mL n-hexane and 1-μL internal standard solution (heptadecanoic acid methyl ester) and was injected into the GC at a temperature of 50°C. After holding for 1 min, the GC's oven was heated at a rate of 8°C/min to 220°C and held for 9 min; then it was heated at 5°C/min rate to 250°C and held for 15 min. Hydrogen was a carrier gas. The injector and the FID were set at an operating temperature of 260°C. The ester content (Y) expressed as a mass fraction in percentage was calculated using the following formula:

$$Y = \frac{\text{area of all FAME} \times \text{weight of internal standard}}{\text{area of internal standard} \times \text{weight of biodiesel sample}} \times 100\%. \quad (2)$$

3. RESULTS AND DISCUSSION

3.1. XRD Analysis

Figure 1 shows the XRD patterns of the catalysts synthesized by different preparation methods. All samples are seen to exhibit low crystallinity and high dispersity of CaO particles. CA-**I** and CA-**S** show an amorphous structure, low intensity of CaO peaks, and no diffraction peaks from CaO-doped alumina [25]. The CA-**P** catalyst shows higher crystallinity of calcium oxide [32, 33]. However, CA-**M** only displays the diffusion of CaO into the alumina structure. This catalyst also shows the presence of $CaAl_2O_4$ (JCPDS 70-0134) which could be associated due to excessive heat generated during the MW-assisted SCS proess. Furthermore, additional peaks corresponding to alumina and/or calcium aluminate hydrate at 2θ of 28.7 and 36.7° illustrate a higher crystallization degree [34]. These structures are formed due to rapid hydration and carbonation of CaO in contact with ambient air [35].

Figure 2 shows the XRD patters of KOH-containing Ca/Al mixed oxides prepared in different routes. All samples have the same diffraction pattern but with different and high crystallinity. Calcium aluminate $Ca_{12}Al_{14}O_{33}$ is present in its cubic structure (JCPDS 48-1882). The transformation of support from $CaAl_2O_4$ to $Ca_{12}Al_{14}O_{33}$ can be related to calcination of KOH-containing calcium aluminate and/or loading of potassium components [36]. Diffusion of Ca ions in the support structure favors the formation of $Ca_3Al_2O_6$ and $C_{12}A_7$ at the expense of CA and C_3A, respectively [37, 38]. The samples demonstrate the formation of a solid solution in which the K^+ cations are highly dispersed over the calcium aluminate lattice without segregation [35]. The samples show distinct peaks of

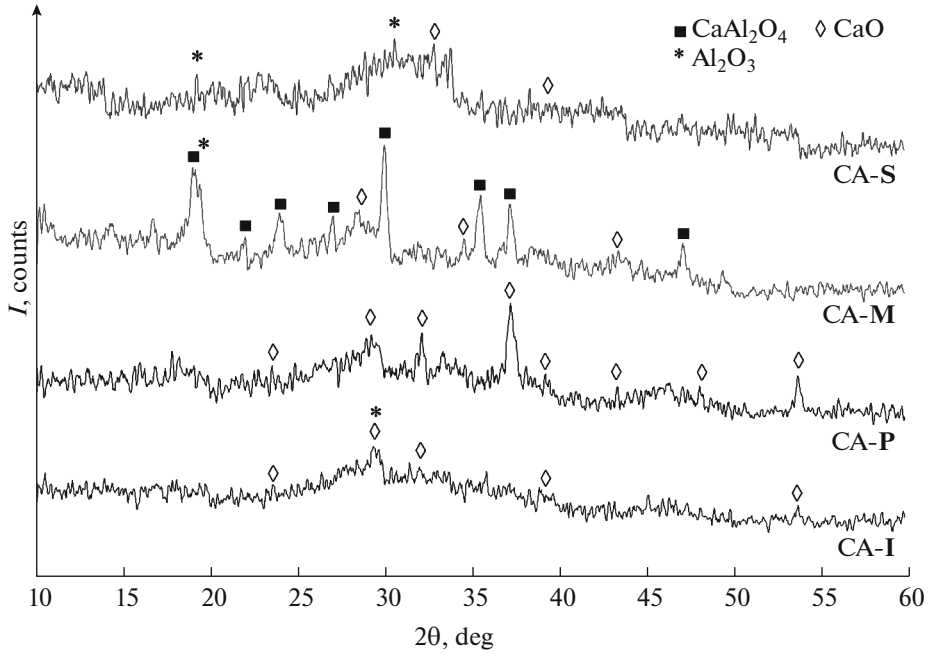

Fig. 1. XRD patterns of CaO–Al_2O_3 catalysts prepared by different methods.

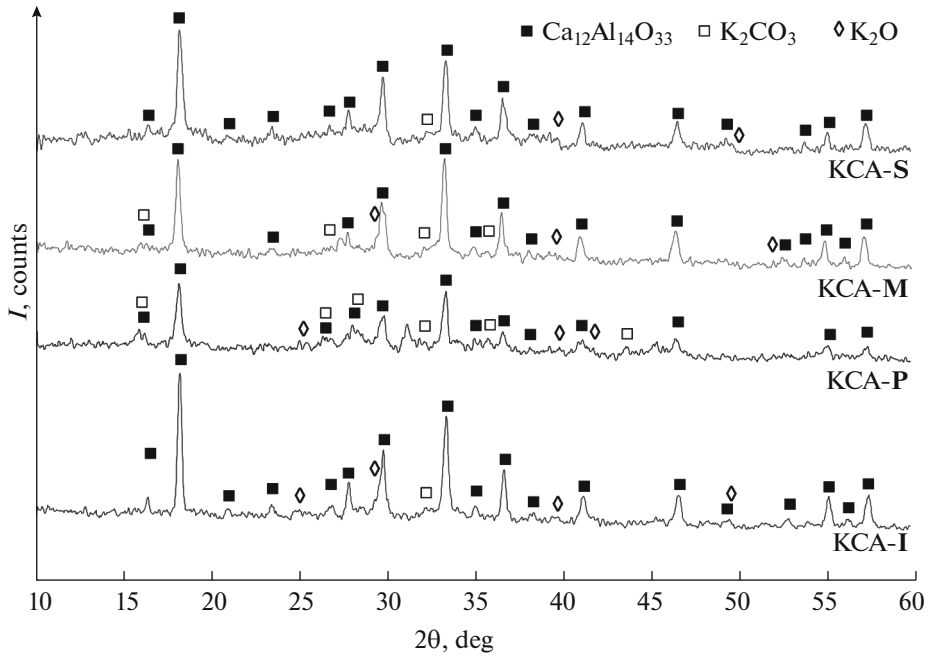

Fig. 2. XRD patterns of KOH/$Ca_{12}Al_{14}O_{33}$ nanocatalysts prepared by different methods.

potassium ions from calcium oxide originating from K_2CO_3 [32].

The physicochemical properties of synthesized catalysts are collected in Table 1. The crystalline size of KCA-**S** and KCA-**I** (derived from strong peaks at 2θ = 18.1°) a smallest and largest values, respectively. Moreover, The KCA-**P** nanocatalyst showeds the lowest relative crystallinity.

3.2. BET/BJH Results, Basicity, and Catalytic Activity

BET/BJH properties of samples are listed in Table 1. The CA-**P** sample has the highest surface area (S_a) and high pore volume (P_v). However, the CA-**M** catalyst showed the largest mean pore size (P_d), which can be related to the egression of high amount of smoke during catalyst preparation. It is reported that catalysts

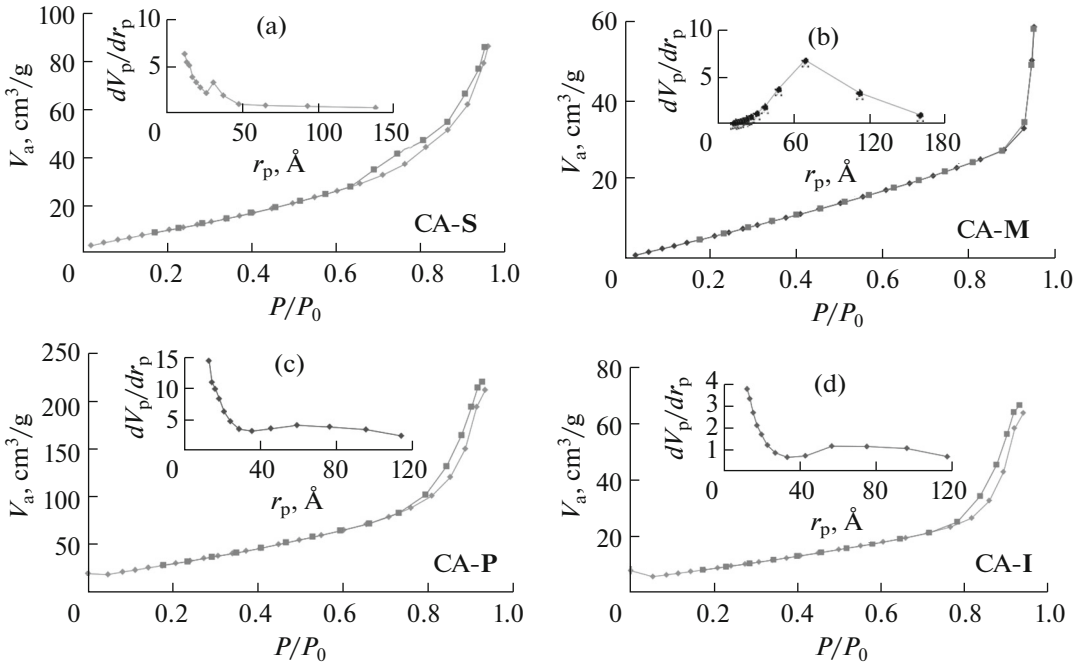

Fig. 3. The curves of N_2 adsorption–desorption hysteresis and pore size distribution plots for the catalysts under consideration.

must have a pore size greater than 6 nm for permeation of large triglycerides molecules inside the pores to show excellent activity in the transesterification reaction [39, 40]. In the presence of KOH loading, the surface area and pore volume of CA-**S** and CA-**P** catalysts markedly decreased while those of CA-**M** and CA-**I**, increased. Upon penetration of some potassium inside the pores, the mean pore size of all samples slightly decreased.

Figure 3 presents the curves of N_2 adsorption–desorption hysteresis and pore size distribution plots for the catalysts under consideration. According to IUPAC classification, our samples show a characteristic type IV curve typical of mesoporous materials. The hysteresis loops of CA-**P** and CA-**I** samples are close to H1 type corresponding to pores of cylindrical shape. However, the CA-**M** and CA-**S** catalysts show a loop of H3 type inherent to plate-like particles and slit-shaped pores [41]. The CA–**M** catalyst exhibits a wide pore size distribution as compared to other samples due to advantages of SCS method. The hysteresis plots for $KOH/Ca_{12}Al_{14}O_{33}$ catalysts (not shown here) has a shape of type IV curve (H3 type). The KCA-**M** catalyst shows a wide pore size distribution which favors its activity in the transesterification reaction.

As is seen in Table 1, samples of the CA series show the basicity of <7.2 while those of the KCA series, within the range 9.8–15. Although the basicity of samples was similar, the FAME content of reaction product of canola oil with methanol catalyzed by each individual catalyst was different. It can be assigned to different pores size of nanocatalysts, which plays a key role in transesterification reaction. For a narrow-pore catalyst (mean pore diameter about 4 nm), a 50-% decrease in catalytic activity could be expected [40] relative to the activity of catalysts with medium ($d \approx 6$ nm) and wide pores ($d \approx 8$ nm). Therefore, the KCA-**M** nanocatalyst exhibited higher activity: around 86% of canola oil was converted to biodiesel.

3.3. SEM/EDX Results

SEM images of the KCA nanocatalysts are given in Fig. 4. All samples exhibit the calcium aluminate phase with a nanorod-like structure [42]. The nanorods are 300–1000 nm long and 30–60 nm wide. The KCA-**S** catalyst shows agglomerated particles with irregular growth of calcium aluminate nanorods. The SCS-produced catalyst (Fig. 4b) shows a more uniform structure that could provide appropriate surface area to perching the active sites (potassium components) to the catalyst surface. The KCA-**P** nanocatalyst (Fig. 4d) consists of agglomerated particles, which decreased its surface area and pore size and could be a reason for low activity of the catalyst. KCA-**I** shows a lumpy structure with non-uniformly grown calcium aluminate nanorods.

The atomic-weight contents of KCA catalysts are summarized in Table 2. As could be expected, all samples contained only Al, Ca, K and O, and no contaminating elements. The weight ratios of Ca and K to Al are larger in case of KCA-**M** catalyst (Table 2). This could be due to good crystallinity of KCA-M, which promotes the adsorption of higher amount of KOH to

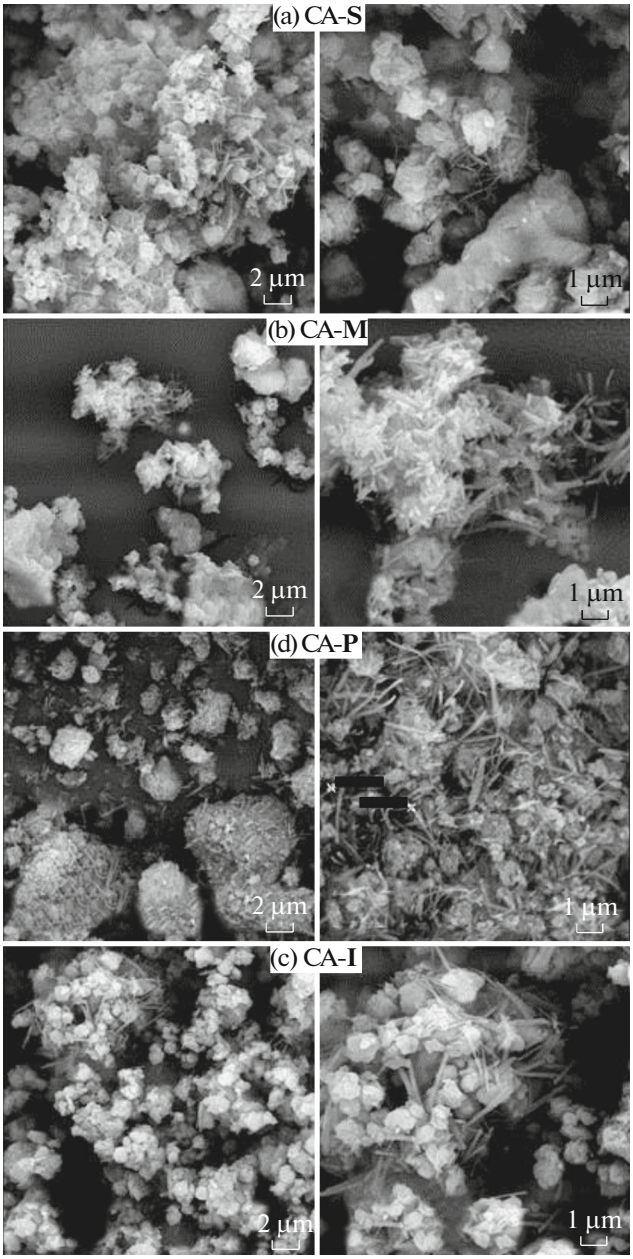

Fig. 4. SEM images of $KOH/Ca_{12}Al_{14}O_{33}$ catalysts prepared by different methods.

the surface and the diffusion of calcium into the alumina structure.

The EDX dot-mapping image of the KCA-M nanocatalyst is shown in Fig. 5. The elements are uniformly distributed and the results good agree with the SEM/EDX data. It can be concluded that MW-assisted SCS is an attractive route for preparation of nanocatalysts with the elements ratios close to the nominal ones, high surface area, porous structure, and the metal oxides incorporated uniformly into the oxide-based matrix.

3.4. FTIR Spectra

The FTIR spectra of SCS-produced catalysts are presented in Fig. 6. The spectrum of pristine Al_2O_3 (curve 5a) shows major bands at 400–550 and 600–800 cm^{-1} attributed to vibrational modes of AlO_6 and AlO_4, respectively. The band around 1385 cm^{-1} was assigned to stretching vibrations of Al–O groups [43]. Addition of CaO to alumina gave birth to new bands below 1000 cm^{-1} (curve 5b). The peaks in the ranges 600–800 and 1400–1500 cm^{-1} can be associated with formation of mono and bidentate carbonates. The intense bands at wavenumbers below 600 cm^{-1} can be assigned to the vibrational modes of CaO [44, 45]. The stretching vibrations of surface hydroxyl groups (Ca–OH) and physisorbed moisture manifest themselves in the range 3200–3600 cm^{-1} [20]. The KCA-M catalyst (curve 5c) exhibits some vibrational bands in the range 3200–3600 cm^{-1}. Shahraki et al. [46] assigned them to stretching vibration of Al–O–K groups that form upon the attachment of K^+ ions to alumina during the activation process. The same peak was observed at 1100 cm^{-1}, which led to the conclusion that the surface Al–O–K groups probably are the main active sites. In addition, the shape of peaks in the ranges 400–600 and 600–800 cm^{-1} became sharper with the formation of a bond between calcium oxide and aluminum oxide to yield calcium aluminate. The band around 1636 cm^{-1} was assigned to the bending mode of the O–H bond of physically adsorbed water [21].

Table 2. EDX results for $KOH/Ca_{12}Al_{14}O_{33}$ catalysts prepared by different methods

	Atomic %				Weight %					
	Al	Ca	K	O	Al	Ca	K	O	Ca/A	K/Al
KCA-S	14.7	9.0	10.6	65.7	17.8	16.1	18.7	47.4	0.90	1.05
KCA-M	12.1	11.0	8.8	68.1	14.9	20	15.6	49.5	1.34	1.05
KCA-P	16.7	9.7	9.4	64.2	20.2	17.4	16.5	45.9	0.86	0.82
KCA-I	15.8	12.6	8.2	63.4	18.8	22.3	14.2	44.7	1.19	0.76

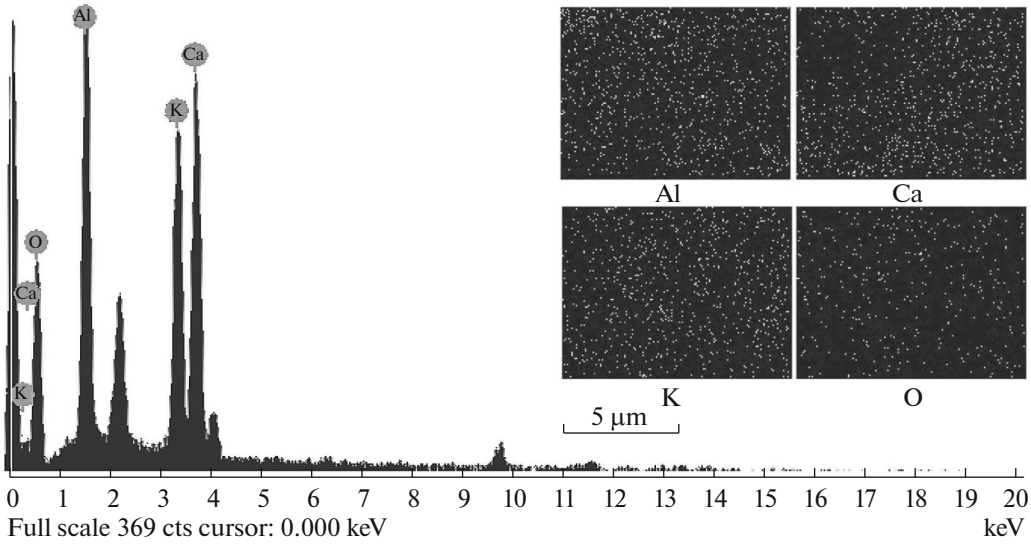

Fig. 5. The EDX dot-mapping image of KCA-**M** nanocatalyst.

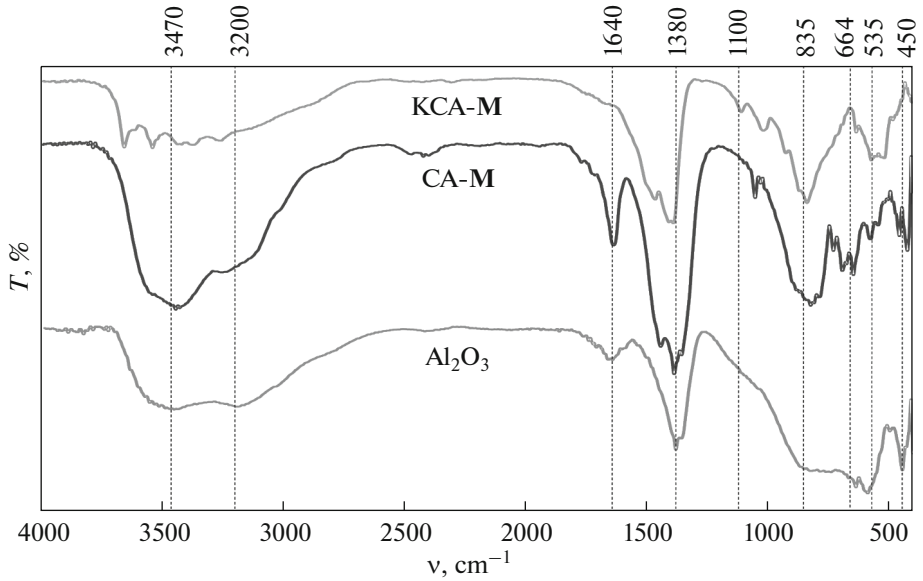

Fig. 6. FTIR spectra of (a) Al_2O_3, (b) $CaAl_2O_4$, and (c) $KOH/Ca_{12}Al_{14}O_{33}$ prepared by microwave-assisted solution combustion synthesis.

3.5. Reusability of KCA-M Catalyst

The reusability of KCA-**M** catalyst in the transesterification reaction is characterized in Fig. 7. After the reaction, the sample was washed twice with methanol and used in second reaction after calcination at 700°C for 1 h because of the egression of reactants and/or products from the pores and surface, as suggested by Zabeti et al. [17]. The catalyst showed good stability in the transesterification: it retained its performance on a level of 75% after at least four cycles. The as-synthesized nanocatalyst exhibited high activity and stability in transesterification reaction and deserve further studies toward industrial application of the process.

4. CONCLUSIONS

In this study, calcium aluminate was applied in the transesterification reaction. The applicability and economic efficiency of different methods for synthesizing catalysts—such as sol–gel, co-precipitation, impregnation, MW-assisted SCS,—were assessed. The

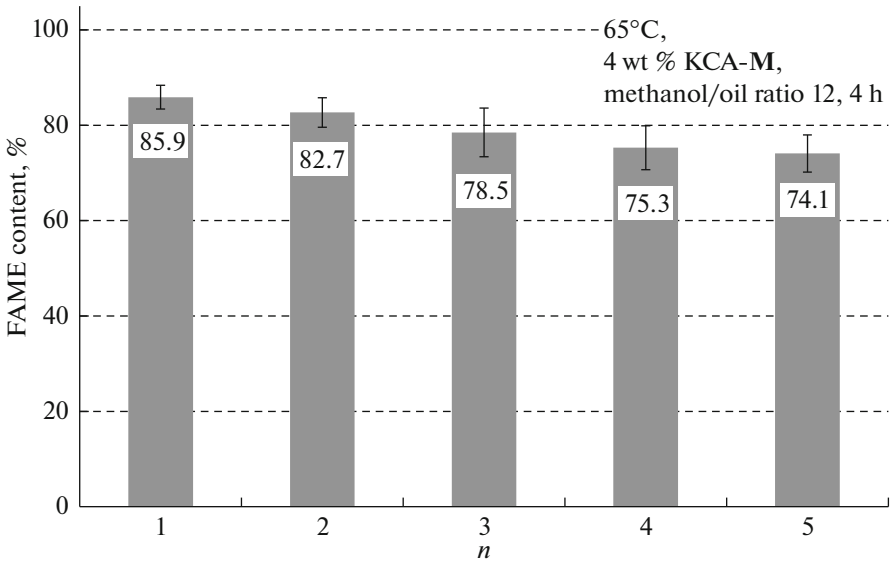

Fig. 7. Reusability of KOH/$Ca_{12}Al_{14}O_{33}$ nanocatalyst (KCA-**M**) prepared by MW-assisted SCS: FAME content vs. number of cycles *n*.

$CaO–Al_2O_3$ mixed oxide prepared by M-SCS showed higher crystallinity compared to other techniques. Upon impregnation with KOH, the monocalcium aluminate undergoes phase transition into a mayenite structure due to diffusion of calcium component into the alumina lattice. This phenomenon was also observed and for the other samples. The nanocomposite synthesized by M-SCS shows higher pore size, basicity, and activity in transesterification reaction (86% yields) compared to the catalysts prepared by other methods. Therefore, M-SCS method can be readily recommended for preparation of nanocatalyst with high surface area, porosity, activity, and stability.

ACKNOWLEDGMENTS

This work was financially supported by the Ferdowsi University of Mashhad (grant no. 32009) and also by the Iran Nanotechnology Initiative Council for complementary financial supports (grant no. 80968).

REFERENCES

1. Abbaszaadeh, A., Ghobadian, B., Omidkhah, M.R. and Najafi, G., Current biodiesel production technologies: A comparative review, *Energy Conv. Manage.,* 2012, vol. 63, pp. 138–148. doi 10.1016/j.enconman.2012.02.027
2. Jeenpadiphat, S. and Tungasmita, D.N., Acid-activated pillar bentonite as a novel catalyst for the esterification of high FFA oil, *Powder Technol.,* 2013, vol. 237, pp. 634–640. doi 10.1016/j.powtec.2013.02.001
3. Borges, M.E. and Diaz, L., Recent developments on heterogeneous catalysts for biodiesel production by oil esterification and transesterification reactions: A review, *Renewable Sustain. Energy Rev.,* 2012, vol. 16, no. 5, pp. 2839–2849. doi 10.1016/j.rser.2012.01.071
4. Atadashi, I.M., Aroua, M.K., Abdul Aziz, A.R., and Sulaiman, N.M.N., The effects of catalysts in biodiesel production: A review, *J. Ind. Eng. Chem.,* 2013, vol. 19, no. 1, pp. 14–26. doi 10.1016/j.jiec.2012.07.009
5. Komintarachat, C. and Chuepeng, S., Solid acid catalyst for biodiesel production from waste used cooking oils, *Ind. Eng. Chem. Res.,* 2009, vol. 48, no. 20, pp. 9350–9353. doi 10.1021/ie901175d
6. Vyas, A.P., Subrahmanyam, N. and Patel, P.A., Production of biodiesel through transesterification of Jatropha oil using KNO_3/Al_2O_3 solid catalyst, *Fuel,* 2009, vol. 88, no. 4, pp. 625–628. doi 10.1016/j.fuel.2008.10.033
7. Arzamendi, G., Campo, I., Arguiñarena, E., Sánchez, M., Montes, M. and Gandia, L.M., Synthesis of biodiesel with heterogeneous NaOH/alumina catalysts: Comparison with homogeneous NaOH, *Chem. Eng. J.,* 2007, vol. 134, nos. 1–3, pp. 123–130. doi 10.1016/j.cej.2007.03.049
8. Taufiq-Yap, Y.H., Abdullah, N.F., and Basri, M., Biodiesel production via transesterification of palm oil using $NaOH/A1_2O_3$ catalysts, *Sains Malays.,* 2011, vol. 40, no. 6, pp. 587–594.
9. Teo, S.H., Taufiq-Yap, Y.H., and Ng, F.L., Alumina supported/unsupported mixed oxides of Ca and Mg as heterogeneous catalysts for transesterification of *Nannochloropsis* sp. *microalga's* oil, *Energy Conv. Manage.,* 2014, vol. 88, pp. 1193–1199. doi 10.1016/j.enconman.2014.04.049
10. Wang, R., Yang, S., Yin, S., Song, B., Bhadury, P., Xue, W., Tao, S., Jia, Z., Liu, D., and Gao, L., Development of solid base catalyst X/Y/MgO/γ-Al_2O_3 for optimization of preparation of biodiesel from *Jatropha curcas* L. seed oil, *Front. Chem. Eng. China,* 2008, vol. 2, no. 4, pp. 468–472.

11. Sankaranarayanan, T.M., Pandurangan, A., Banu, M., and Sivasanker, S., Transesterification of sunflower oil over MoO_3 supported on alumina, *Appl. Catal. A,* 2011, vols. 409–410, pp. 239–247. doi 10.1016/j.apcata.2011.10.013

12. Amani, H., Ahmad, Z., Asif, M., and Hameed, B.H., Transesterification of waste cooking palm oil by MnZr with supported alumina as a potential heterogeneous catalyst, *J. Ind. Eng. Chem.,* 2014, vol. 20, no. 6, pp. 4437–4442. doi 10.1016/j.jiec.2014.02.012

13. Benjapornkulaphong, S., Ngamcharussrivichai, C., and Bunyakiat, K., Al_2O_3-supported alkali and alkali earth metal oxides for transesterification of palm kernel oil and coconut oil, *Chem. Eng. J.,* 2009, vol. 145, no. 3, pp. 468–474. doi 10.1016/j.cej.2008.04.036

14. Umdu, E.S., Tuncer, M., and Seker, E., Transesterification of *Nannochloropsis oculata microalga*'s lipid to biodiesel on Al_2O_3 supported CaO and MgO catalysts, *Bioresour. Technol.,* 2009, vol. 100, no. 11, pp. 2828–2831. doi 10.1016/j.biortech.2008.12.027

15. Umdu, E.S. and Seker, E., Transesterification of sunflower oil on single step sol–gel made Al_2O_3 supported CaO catalysts: Effect of basic strength and basicity on turnover frequency, *Bioresour. Technol.,* 2012, vol. 106, no. 2, pp. 178–181. doi 10.1016/j.biortech.2011.11.135

16. Zabeti, M., Daud, W.M.A.W., and Aroua, M.K., Optimization of the activity of CaO/Al_2O_3 catalyst for biodiesel production using response surface methodology, *Appl. Catal. A,* 2009, vol. 366, no. 1, pp. 154–159. doi 10.1016/j.apcata.2009.06.047

17. Zabeti, M., Daud, W.M.A.W., and Aroua, M.K., Biodiesel production using alumina-supported calcium oxide: An optimization study, *Fuel Process. Technol.,* 2010, vol. 91, no. 2, pp. 243–248. doi 10.1016/j.fuproc.2009.10.004

18. Noiroj, K., Intarapong, P., Luengnaruemitchai, A., and Jai-In, S., A comparative study of KOH/Al_2O_3 and KOH/NaY catalysts for biodiesel production via transesterification from palm oil, *Renewable Energy,* 2009, vol. 34, no. 4, pp. 1145–1150. doi 10.1016/j.renene.2008.06.015

19. Hájek, M., Skopal, F., Čapek, L., Černoch, M., and Kutálek, P., Ethanolysis of rapeseed oil by KOH as homogeneous and as heterogeneous catalyst supported on alumina and CaO, *Energy,* 2012, vol. 48, no. 1, pp. 392–397. doi 10.1016/j.energy.2012.06.052

20. Liao, C.-C. and Chung, T.-W., Optimization of process conditions using response surface methodology for the microwave-assisted transesterification of Jatropha oil with KOH impregnated CaO as catalyst, *Chem. Eng. Res. Des.,* 2013, vol. 91, no. 12, pp. 2457–2464. doi 10.1016/j.cherd.2013.04.009

21. Xie, W., Peng, H. and Chen, L., Transesterification of soybean oil catalyzed by potassium loaded on alumina as a solid-base catalyst, *Appl. Catal. A,* 2006, vol. 300, no. 1, pp. 67–74. doi 10.1016/j.apcata.2005.10.048

22. Ma, G., Hu, W., Pei, H., Jiang, L., Ji, Y., and Mu, R., Study of KOH/Al_2O_3 as heterogeneous catalyst for biodiesel production via in situ transesterification from microalgae, *Environ. Technol.,* 2014, vol. 36, no. 5, pp. 622–627. doi 10.1080/09593330.2014.954629

23. Yan, S., Lu, H., and Liang, B., Supported CaO catalysts used in the transesterification of rapeseed oil for the purpose of biodiesel production, *Energy Fuels,* 2007, vol. 22, no. 1, pp. 646–651. doi 10.1021/ef070105o

24. Moradi, G., Mohadesi, M., Rezaei, R., and Moradi, R., Biodiesel production using $CaO/\gamma\text{-}Al_2O_3$ catalyst synthesized by sol-gel method, *Can. J. Chem. Eng.,* 2015, vol. 93, no. 9, pp. 1531–1538. doi 10.1002/cjce.22258

25. Mahdavi, V. and Monajemi, A., Optimization of operational conditions for biodiesel production from cottonseed oil on $CaO–MgO/Al_2O_3$ solid base catalysts, *J. Taiwan Inst. Chem. Eng.,* 2014, vol. 45, no. 5, pp. 2286–2292. doi 10.1016/j.jtice.2014.04.020

26. Zhou, H., Sun, J., Ren, B., Wang, F., Wu, X., and Bai, S., Effects of alkaline media on the controlled large mesopore size distribution of bimodal porous silicas via sol–gel methods, *Powder Technol.,* 2014, vol. 259, pp. 46–51. doi 10.1016/j.powtec.2014.03.060

27. González, E.A.Z., García-Guaderrama, M., Villalobos, M.R., Dellamary, F.L., Kandhual, S., Rout, N.P., Tiznado, H., and Arizaga, G.G.C., Potassium titanate as heterogeneous catalyst for methyl transesterification, *Powder Technol.,* 2015, vol. 280, pp. 201–206. doi 10.1016/j.powtec.2015.04.030

28. López-Delgado, A., López, F.A., Gonzalo-Delgado, L., López-Andrés, S., and Alguacil, F.J., Study by DTA/TG of the formation of calcium aluminate obtained from an aluminum hazardous waste, *J. Therm. Anal. Calorim.,* 2009, vol. 99, no. 3, pp. 999–1004. doi 10.1007/s10973-009-0597-z

29. Hashemzehi, M., Saghatoleslami, N., and Nayebzadeh, H., A study on the structure and catalytic performance of $Zn_xCu_{1-x}Al_2O_4$ catalysts synthesized by the solution combustion method for the esterification reaction, *C. R. Acad. Sci. Chim.,* 2016, vol. 19, no. 8, pp. 955–962. doi 10.1016/j.crci.2016.05.006

30. Ebadzadeh, T. and Asadian, K., Microwave-assisted synthesis of nanosized $\alpha\text{-}Al_2O_3$, *Powder Technol.,* 2009, vol. 192, no. 2, pp. 242–244. doi 10.1016/j.powtec.2009.01.001

31. Ye, B., Qiu, F., Sun, C., Li, Y., and Yang, D., Biodiesel production from soybean oil using heterogeneous solid base catalyst, *J. Chem. Technol. Biotechnol.,* 2014, vol. 89, no. 7, pp. 988–997. doi 10.1002/jctb.4190

32. Yang, L., Lv, P., Yuan, Z., Luo, W., Li, H., Wang, Z., and Miao, C., Synthesis of biodiesel by different carriers supported KOH catalyst, *Adv. Mater. Res.,* 2012, vols. 581–582, pp. 197–201. doi 10.4028/www.scientific.net/AMR.581-582.197

33. Pasupulety, N., Gunda, K., Liu, Y., Rempel, G.L., and Ng, F.T.T., Production of biodiesel from soybean oil on CaO/Al_2O_3 solid base catalysts, *Appl. Catal. A,* 2013, vol. 452, no. 1, pp. 189–202. doi 10.1016/j.apcata.2012.10.006

34. Toniolo, J.C., Lima, M.D., Takimi, A.S., and Bergmann, C.P., Synthesis of alumina powders by the glycine–nitrate combustion process, *Mater. Res. Bull.,* 2005, vol. 40, no. 3, pp. 561–571. doi 10.1016/j.materresbull.2004.07.019

35. Castro, C.S., Garcia Júnior, L.C.F., and Assaf, J.M., The enhanced activity of Ca/MgAl mixed oxide for

transesterification, *Fuel Process. Technol.,* 2014, vol. 125, pp. 73–78. doi 10.1016/j.fuproc.2014.03.024

36. Ruszak, M., Witkowski, S., Pietrzyk, P., Kotarba, A., and Sojka, Z., The role of intermediate calcium aluminate phases in solid state synthesis of mayenite ($Ca_{12}Al_{14}O_{33}$), *Funct. Mater. Lett.,* 2011, vol. 4, no. 2, pp. 183–186. doi 10.1142/S1793604711001907
37. Boysen, H., Kaiser-Bischoff, I., Lerch, M., Berendts, S., Hoelzel, M., and Senyshyn, A., Disorder and diffusion in mayenite, *Acta Phys. Pol.,* 2010, vol. 117, no. 1, pp. 38–41. doi 10.12693/APhysPolA.117.38
38. Avci, N., Korthout, K., Newton, M.A., Smet, P.F., and Poelman, D., Valence states of europium in $CaAl_2O_4$:Eu phosphors, *Opt. Mater. Express,* 2012, vol. 2, no. 3, pp. 321–330.
39. Rahmani Vahid, B. and Haghighi, M., Urea–nitrate combustion synthesis of MgO/$MgAl_2O_4$ nanocatalyst used in biodiesel production from sunflower oil: Influence of fuel ratio on catalytic properties and performance, *Energy Conv. Manage.,* 2016, vol. 126, pp. 362–372. doi 10.1016/j.enconman.2016.07.050
40. Jacobson, K., Gopinath, R., Meher, L.C., and Dalai, A.K., Solid acid catalyzed biodiesel production from waste cooking oil, *Appl. Catal. B,* 2008, vol. 85, nos. 1–2, pp. 86–91. doi 10.1016/j.apcatb.2008.07.005
41. Shao, G.N., Sheikh, R., Hilonga, A., Lee, J.E., Park, Y.-H., and Kim, H.T., Biodiesel production by sulfated mesoporous titania–silica catalysts synthesized by the sol–gel process from less expensive precursors, *Chem. Eng. J.,* 2013, vols. 215–216, pp. 600–607. doi 10.1016/j.cej.2012.11.059
42. Chang, Y.-P., Chang, P.-H., Lee, Y.-T., Lee, T.-J., Lai, Y.-H., and Chen, S.-Y., Morphological and structural evolution of mesoporous calcium aluminate nanocomposites by microwave-assisted synthesis, *Micropor. Mesopor. Mater.,* 2014, vol. 183, pp. 134–142. doi 10.1016/j.micromeso.2013.09.013
43. Meng, Y.-L., Wang, B.-Y., Li, S.-F., Tian, S.-J., and Zhang, M.-H., Effect of calcination temperature on the activity of solid Ca/Al composite oxide-based alkaline catalyst for biodiesel production, *Bioresour. Technol.,* 2013, vol. 128, no. 2, pp. 305–309. doi 10.1016/j.biortech.2012.10.152
44. Alba-Rubio, A.C., Santamaría-González, J., Mérida-Robles, J.M., Moreno-Tost, R., Martín-Alonso, D., Jiménez-López, A., and Maireles-Torres, P., Heterogeneous transesterification processes by using CaO supported on zinc oxide as basic catalysts, *Catal. Today,* 2010, vol. 149, nos. 3–4, pp. 281–287. doi 10.1016/j.cattod.2009.06.024
45. Albuquerque, M.C.G., Azevedo, D.C.S., Cavalcante, C.L., Jr., Santamaría-González, J., Mérida-Robles, J.M., Moreno-Tost, R., Rodríguez-Castellón, E., Jiménez-López, A., and Maireles-Torres, P., Transesterification of ethyl butyrate with methanol using MgO/CaO catalysts, *J. Mol. Catal. A,* 2009, vol. 300, nos. 1–2, pp. 19–24. doi 10.1016/j.molcata.2008.10.033
46. Shahraki, H., Entezari, M.H., and Goharshadi, E.K., Sono-synthesis of biodiesel from soybean oil by KF/γ-Al_2O_3 as a nano-solid-base catalyst, *Ultrason. Sonochem.,* 2015, vol. 23, pp. 266–274. doi 10.1016/j.ultsonch.2014.09.010